

Theoretical models of catalytic domains of protein phosphatases 1 and 2A with Zn^{2+} and Mn^{2+} metal dications and putative bioligands in their catalytic centers[★]

Edyta Woźniak-Celmer, Stanisław Ołdziej and Jerzy Ciarkowski[✉]

Faculty of Chemistry, University of Gdańsk, Gdańsk, Poland

Received: 2 November, 2000; revised: 31 January, 2001; accepted: 3 March, 2001

Key words: protein phosphatase 1A and 2B, protein phosphatase inhibitors, homology modeling, constrained simulated annealing, molecular dynamics

The oligomeric metalloenzymes protein phosphatases dephosphorylate OH groups of Ser/Thr or Tyr residues of proteins whose actions depend on the phosphorus signal. The catalytic units of Ser/Thr protein phosphatases 1, 2A and 2B (PP1c, PP2Ac and PP2Bc, respectively), which exhibit about 45% sequence similarity, have their active centers practically identical. This feature strongly suggests that the unknown structure of PP2Ac could be successfully homology-modeled from the known structures of PP1c and/or PP2Bc. Initially, a theoretical model of PP1c was built, including a phosphate and a metal dication in its catalytic site. The latter was modeled, together with a structural hydroxyl anion, as a triangular pseudo-molecule (Zno or Mno), composed of two metal cations (double Zn^{2+} or Mn^{2+} , respectively) and the OH^- group. To the free PP1c two inhibitor sequences $R^{29}RRRPpTPAMLFR^{40}$ of DARPP-32 and $R^{30}RRRPpTPATLVLT^{42}$ of Inhibitor-1, and two putative substrate sequences LRRApSVA and QRRQRKpRRTI were subsequently docked. In the next step, a free PP2Ac model was built *via* homology re-modeling of the PP1c template and the same four sequences were docked to it. Thus, together, 20 starting model complexes were built, allowing for combination of the Zno and Mno pseudo-molecules, free enzymes and the peptide ligands docked in the catalytic sites of PP1c and PP2Ac. All models were subsequently subjected to 250–300 ps molecular dynamics using the AMBER 5.0 program. The equilibrated trajectories of the final 50 ps were taken for further analyses. The theoretical models of PP1c complexes, irrespective of the dication type, exhibited increased mobilities in the following residue ranges: 195–200, 273–278, 287–209 for the inhibitor sequences and 21–25, 194–200, 222–227,

[★] Presented at the International Conference on “Conformation of Peptides, Proteins and Nucleic Acids”, Debrzyno, Poland, 2000.

[✉] Supported by grants BW/8000-5-0241-0 and 3 T09A 045 19 from the State Committee for Scientific Research (KBN, Poland). The computations were carried out at the Academic Computer Center in Gdańsk TASK, Poland, and the Interdisciplinary Center for Mathematical Modeling (ICM) in Warsaw, Poland.

[✉] Correspondence: Jerzy Ciarkowski, Faculty of Chemistry, University of Gdańsk, J. Sobieskiego 18, 80-952, Gdańsk, Poland; tel. (48 58) 345 0330; fax: (48 58) 341 0357; e-mail: jurek@chemik.chem.univ.gda.pl

Abbreviations: PDB, Protein Data Bank; MD, molecular dynamics; MO, molecular orbital(s); PP, protein phosphatase; PP1c, PP2Ac, PP2Bc, catalytic units; pT(S), phosphorylated threonine (serine); RMS, root mean square; other abbreviations are defined in the text, where applicable.

261, 299–302 for the substrate sequences. Paradoxically, the analogous PP2Ac models appeared much more stable in similar simulations, since only their “prosegment” residues 6–10 and 14–18 exhibited an increased mobility in the inhibitor complexes while no areas of increased mobility were found in the substrate complexes. Another general observation was that the complexes with Mn dications were more stable than those with Zn dications for both PP1c and PP2Ac units.

The reversible phosphorylation/dephosphorylation of proteins by protein kinases/phosphatases is the most important switch in the regulation of a majority of cellular activities, from growth and metabolism to memory. Unlike the kinases, all showing a uniform structure, there are several families of protein phosphatases (PP) with little or no sequence and structural mutual homology (Jia, 1997). Thus, the eukaryotic protein tyrosine phosphatases differ from the serine/threonine phosphatases, which further subdivide into subclasses (Barford, 1996). Initially, the serine/threonine phosphatases were classified into four groups PP1, PP2A, PP2B and PP2C on the basis of differences in their biochemical properties (Ingebritsen & Cohen, 1983). To date it is known that the functional enzymes work in hetero-associates, composed of the catalytic subunit and one or more variable regulatory subunits, which are tissue dependent and a target substrate (Barford, 1996; Żolnierowicz & Hemmings, 1996; Cohen, 1997; Klee *et al.*, 1998; Berndt, 1999; Millward *et al.*, 1999; Aggen *et al.*, 2000). It is also known that the catalytic units of PP1, PP2A and PP2B (PP1c, PP2Ac and PP2Bc, respectively) are homologous in sequence, structure and mechanism of action, and differ from that of PP2C (Barford, 1996; Jia, 1997; Herzig & Neuman, 2000). The latter differences were evidenced by experiments on solution of PP1c structure (Egloff *et al.*, 1995; 1997; Goldberg *et al.*, 1995), PP2B (Griffith *et al.*, 1995; Kissinger *et al.*, 1995) and PP2C (Das *et al.*, 1996).

The PP1 and PP2B catalytic subunits consist of a central β sandwich made of a sheet of six β strands, covered by three α helices and three other β strands on the lower side, and a sheet of five β strands, covered on its top by an all-helical domain. The two metal ions, separated by about 3.5 Å, are coordinated by a phosphate and several strictly conserved His, Asp, Asn and Arg residues provided by the two faces of the β sandwich. To-

gether, they define the deeply nested catalytic center, flanked from its upper side by a unique $\beta\alpha\beta\alpha\beta$ scaffold, comprising three β strands from the upper slice of the β sandwich and two α helices from the all-helical domain (Fig. 1).

A fairly long substrate trench, kinked by about 120° in its midpoint at the PP1c active center and thus divided into a pre-phosphorylation N-terminal part and a post-phosphorylation C-terminal section, is incoming from the south-east and continuing to the west (Fig. 1). In PP1c the N-terminal groove is highly acidic and the C-terminal groove is hydrophobic yet this is not the case in the homologous PP2Ac and PP2Bc (Goldberg *et al.*, 1995). The reported PP1c and PP2Bc structures contain iron, manganese and/or zinc ions, depending on crystallization conditions (Egloff *et al.*, 1995; 1997; Goldberg *et al.*, 1995; Griffith *et al.*, 1995; Kissinger *et al.*, 1995). There is a debate as to what cations support the native PP1, although the most likely candidate is the combination of Zn^{2+} and Fe^{2+} (Chu *et al.*, 1996; Cohen, 1997).

The purpose of this work is an endeavor to study the delicate problem of reliable molecular simulations of the catalytic subunit of serine/threonine phosphatases in particular, and metalloenzymes in general. So far, there are only a few PP1c simulations reported, with the metal dications treated quite crudely, e.g. by Lindvall *et al.* (1997). A simple and workable parameterization and implementation of the metal cations is a particular objective of this project. We propose and test a concept of a triangular pseudo-molecule, made of two metal cations and a structural OH^- so parameterized regarding the geometry, force constants and charges as to adequately mimick the properties of the experimental PP1c complex (Egloff *et al.*, 1995; Barford, 1996). For this test case we have chosen two uniform metal di-cations, *viz.* 2Zn^{2+} and 2Mn^{2+} , easy enough to parameterize, adequate for structure compari-

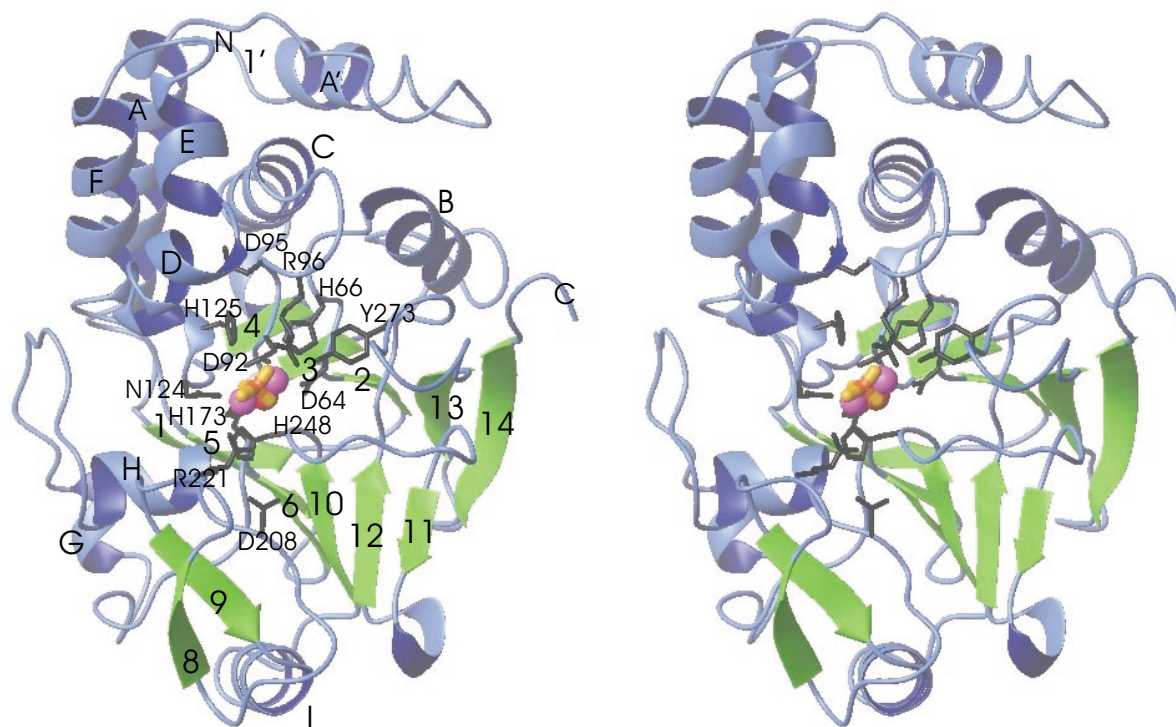


Figure 1. The standard view of PP1c, a stereo diagram.

The figure is based on the structure, deposited as PDB file 1fjm (Goldberg *et al.*, 1995) modified as described in Methods for the starting model of PP1c·Zno·Tpo. The metal cations and the structural OH⁻ are represented as magenta balls while the phosphate (orange) and the conserved residues (see Methods) in the active center (black) are shown as sticks. The secondary structure is defined as in Goldberg *et al.* (1995) and labelled accordingly. The figure was prepared using the Molmol program (Koradi *et al.*, 1996).

sons, and reported to be active *in vitro*, when incorporated into PP1 (Chu *et al.*, 1996). The reason for not including a more realistic combination of both Zn²⁺ and Fe²⁺ (Chu *et al.*, 1996; Cohen, 1997) in a single di-cation is that such a “non-symmetrical” double-metal center is a quite hard case for exact geometry-optimization and subsequent parameterization. Subsequently we studied the effect of these two uniform metal di-cations on binding inhibitor sequences, the phosphorylated dodecapeptide R²⁹RRRPpTPAMLF⁴⁰ (since here on: acronym DAR), a fragment of DARPP-32 (Dopamine- and cyclic AMP-regulated neuronal phosphoprotein; Williams *et al.*, 1986) and the phosphorylated tridecapeptide R³⁰RRRPpTPATLVLT⁴² (acronym I-1) a fragment of inhibitor 1 (Inh-1) (Huang & Glinsmann, 1976).

DARPP-32 (202 amino-acid residues) and Inh-1 (171 residues), although quite differently distributed in mammalian organisms, are mutually homologous, potent and selective protein inhibitors against PP1c and much weaker ones against PP2A and PP2B. A phosphorylated threonine (T34 in DARPP-32 and T-35 in Inh-1) is a prerequisite of their inhibitory activity. Their minor modifications (e.g. pT35D mutation in Inh-1) confer on them a comparative inhibitory power against both PP1 and PP2A (Herzig & Neuman, 2000; Endo *et al.*, 1996). In addition, we also studied the effect of binding of two putative substrate sequences LRRApSVA (acronym 7-pep) and QRRQ-RKpSRRTI (acronym 11-pep), of which the latter is a PP1c substrate while the former is an excellent PP1Ac substrate (Żońmierowicz, personal

communication). It has recently been shown that the sequence around pT³⁴ in DARPP-32 (Kwon *et al.*, 1997; Huang *et al.*, 1999) and pT³⁵ in I-1 (Endo *et al.*, 1996) interacts with PP1c at a site other than the interaction site for the (R/K)(V/I)XF consensus sequence, conserved in all PP1 regulatory units, close to N-termini in DARPP-32 and I-1, whose docking site in PP1c has recently been determined (Egloff *et al.*, 1997) to be in the lower-right hand side of PP1c in Fig. 1, at the external edge of the β -sandwich (not shown). Since it has been further suggested that the sequence surrounding pT in DARPP-32 and/or I-1 may dock in the catalytic cleft of PP1c (Kwon *et al.*, 1997; Huang *et al.*, 1999; Goldberg *et al.*, 1995), we opted to dock all our ligand peptides (the inhibitor and the substrate sequences) in the catalytic trench, where the effect of changing of the metal di-cation(s) could be tested. Since our pseudomolecule test models behaved according to expectations, we intend to extend them, including in future a more realistic combination of Zn²⁺ and Fe²⁺ (Chu *et al.*, 1996; Cohen, 1997) in a single di-cation.

METHODS

Design and parameterization of Zn and Mn residues, the pseudo-molecules composed of $2\text{Zn}^{2+}\cdot\text{OH}^-$ and $2\text{Mn}^{2+}\cdot\text{OH}^-$, respectively; parameterization of the phosphothreonine, Thp, phosphoserine, Sep, and phosphate, Tpo. In accordance with the AMBER philosophy (Case *et al.*, 1997) all newly parameterized molecular fragments (Zno, Mno, Thp, Sep and Tpo) were defined as new units analogous to the amino-acid residues. Zno and Mno were designed, in accordance with the suggestion concluding the paper by Hoops *et al.* (1991), to consist of triangles made of the two metal ions and the oxygen with an exocyclic hydrogen. They have a total charge +3 and an *ab initio*-optimized geometry, very well fitting the PP1c active center. Their Lennard-Jones and force constant parameters were taken from literature (Merz, 1991) or from *ab initio* geometry optimization, as described by Merz (1991) and Hoops *et al.* (1991).

All *ab initio* calculations were done using the GAMESS MO package (Schmidt *et al.*, 1993) and the triple zeta basis set plus *d* polarisation functions on all heavy atoms (Lee *et al.*, 1996). The partial charges for new residues were derived using the RESP (restrained electrostatic potential) procedure (Bayly *et al.*, 1993), as recommended by the AMBER 5.0 manual (Case *et al.*, 1997). For the non-standard residues phosphothreonine, phosphoserine and PO₄³⁻ the force-field (Lennard-Jones, force constants) parameters were taken from the AMBER 5.0 (Case *et al.*, 1997) parameter library while the missing charges were calculated as above, except that the 6-31G^{**} basis set was used for the computation. The resulting new parameters are given in Fig. 2 in the paper by Woźniak *et al.* (2000).

Starting models and simulations for PP1c·Zno·Tpo or PP1c·Mno·Tpo. The chain A of the PP1c structure with a covalently attached marine toxin microcystin at C²⁷³ (Goldberg *et al.*, 1995), deposited in the Brookhaven Protein Data Bank (PDB; Bernstein *et al.*, 1977) in file 1fjm, was chosen as a template for the starting structures of the PP1c with two metal cations and the phosphate in the active center. The removal of microcystin and the copying of the missing PO₄³⁻ from PP2Bc (chain A in file 1tco; Bernstein *et al.*, 1977) onto the active center of PP1c via a superimposition of the PP1c and PP2Bc catalytic centers, have been described in detail by Woźniak *et al.* (2000). Having the PO₄³⁻ (Tpo) configuration copied to the PP1c catalytic center, the two metals plus the structural OH⁻ were defined as a Zno residue (see above) and the free PP1c was initially relaxed to release all intramolecular bad contacts and/or those involving Zno and structural water(s). This relaxation consisted of the first three stages in Table 1, executed *in vacuo*. The most involved stage 2 (the constrained simulated annealing protocol, CSA) was executed using protocols, described in detail elsewhere (Woźniak *et al.*, 2000) with constraints individually customized to each of the analyzed systems. Subsequently, the system was immersed in the box of TIP3P water (Jorgensen *et al.*, 1983) of a size enabling a cutoff for electrostatic interactions at 14 Å, and all consecutive stages (cf. Table 1) were executed until

Table 1. A typical protocol for the molecular dynamics relaxation of the PP1c and PP1Ac starting models, using the AMBER 5.0 package

Steps or ps	Calculation type	Environment	Constraints	Conditions	Dielectrics
20000	Constrained minimization	vacuum	Specific for an enzyme-ligand system; see e.g. (Woźniak <i>et al.</i> , 2000)		distance-dependent
20000	Constrained Simulated annealing	vacuum			distance-dependent
20000	Minimization	vacuum			distance-dependent
20000	Minimization	water		periodic boundary ^{a,b}	1
0–30 ps;	MD	water	as above plus SHAKE on	periodic boundary ^{a,b} ; step 1 fs; npT ensemble ^c	1
30–60 ps;	MD	water	gradually released amino acid distance constraints SHAKE on	periodic boundary ^{a,b} ; step 1 fs; npT ensemble ^c	1
60–90 ps;	MD	water	gradually released Zno(Mno)·phosphate distance constraints SHAKE on	periodic boundary ^{a,b} ; step 1 fs; npT ensemble ^c	1
90–120 ps;	MD	water	None SHAKE on	periodic boundary ^{a,b} ; step 1 fs; npT ensemble ^c	1
120–320 ps;	MD, productive run	water	None SHAKE on	periodic boundary ^{a,b} ; step 2 fs; npT ensemble ^c	1

^aA typical box size was 60 Å × 50 Å × 45 Å, the protein concentration was around 0.125 · 10⁻³ mol · dm⁻³, compatible with about 3300–4500 TIP3P water molecules (Jorgensen *et al.*, 1983), i.e. about 10000–14000 atoms total filling the periodic box; ^bResidue-based cut-off 10–14 Å; ^cp. = 1 at, T=300 K.

full release of the constraints and the final productive molecular dynamics (MD) run. In order to save time, all MD simulations were carried out with frozen carbon–hydrogen covalent bonds (procedure SHAKE; Brooks III *et al.*, 1988). PP1c·Mno·Tpo was obtained by a computer mutation of Zn into Mno, after stage 3 in Table 1, which was then repeated and followed by all consecutive stages.

Starting models and simulations for PP2Ac·Zno·Tpo or PP2Ac·Mno·Tpo. Based on the PP1c, PP2Ac and PP2Bc sequence alignment (Goldberg *et al.*, 1995) and using SYBYL 6.2 (1996) program package, the protein sequence typical of PP1c comprised within the PP1c·(Zno/Mno)·Tpo was computer mutated into that of PP2Ac to give PP2Ac·(Zno/Mno)·Tpo, retaining the molecular architecture of the former. To obtain a full agreement between the

linear and the three-dimensional PP1c-PP2Ac alignment, the first six residues from PP1c were removed and two more deletions (Y¹¹⁴-P¹¹⁵ and K²²¹) and one insertion of G (between Y¹⁴⁴ and N¹⁴⁵) on the PP1c sequence/structure were introduced and the associated strains initially relieved using force field and tools implemented in SYBYL. Six structural water molecules, present in the PP1c experimental template, were removed from the PP2Ac star model. The initial PP2Ac model was superimposed onto the PP1c starting model for control of the agreement of the conserved residues. Further procedures, starting from the next minimalization on, involved AMBER and followed those described for PP1c·Zno·Tpo and PP1c·Mno·Tpo in the former section.

Starting models and simulations for the PP1c·Zno·DAR or PP1c·Mno·DAR com-

plexes. The docking and subsequent simulation procedures are described in detail for the PP1c·Zno·DAR complex taken as a prototype. The dodecapeptide sequence from the PP1c inhibitor/regulatory unit DARPP-32, with the phosphothreonine-34 in the center, R²⁹RRRPpTPAM-LFR⁴⁰ (DAR), was manually docked with the assumption of the maximal complementarity between the substrate cleft and the bioligand (Goldberg *et al.*, 1995). Thus, the RRRR sequence was fitted into the N-terminal acidic section of the cleft, the phosphate from the phosphorylated threonine was constrained exactly to the initial position occupied by the free phosphate (see above), and the consecutive residues were docked into the C-terminal hydrophobic section of the substrate cleft. The precise initial fit was achieved using a combined constrained minimization and constrained simulated annealing (CSA), in accordance with the protocol included in Table 1. The Mno complex was obtained by a computer mutation of Zno into Mno after stage 3 in Table 1. Full relaxation past stage 3 of Table 1 was achieved similarly as for the free PP1c.

Other PP1c and PP2Ac complexes. The starting complexes with other ligands were obtained *via* proper computer mutations of either PP1c·(Zno/Mno)·DAR or PP2Ac·(Zno/Mno)·DAR complexes, followed by CSA with gradually released constraints, carefully selected and typical for each individual case, as described above for the specific example of PP1c·Zno·DAR. Subsequently, the productive simulations were carried out accordingly.

Computations and display. Model building was done using SYBYL (1996) program package. All molecular simulations were done using AMBER 5.0 program (Case *et al.*, 1997) on either the POWER CHALLENGE SGI computer (at the Academic Computer Center in Gdańsk TASK) or T3E computer (at the Interdisciplinary Center for Mathematical and Computational Modeling, ICM, at the University of Warsaw). Figure 1 was prepared using the MOLMOL program (Koradi *et al.*, 1996) Figs. 2 and 4–7 using the PlotMTV program (Toh, 1995) and Fig. 3 using the Rasmol program (Sayle, 1996).

RESULTS

Molecular models of the PP1c and PP2Ac catalytic units

Both our PP1c and PP2Ac models should basically be both compatible with and diverse from their respective twins modeled formerly (Gauss *et al.*, 1997; Aggen *et al.*, 1999). The reason for compatibility is the same strategy of modeling PP2Ac from the PP1c solid state template (Goldberg *et al.*, 1995), taking advantage of their 50% sequence homology. A reason for diversity is the level of relaxation of the models in this work, being far more extensive (including about 210–230 ps unconstrained MD runs at 300K in periodic box filled with water) than in the work quoted (5 ps dynamics/minimization at 300K *in vacuo*, with the enzyme body more than 7–8 Å away from the ligand completely constrained, and the metal ions excised from the catalytic center). Although a direct comparison of the two models is impossible without the respective sets of coordinates, one can believe that the former models of PP1c and PP2Ac must very closely resemble the solid-state structure of PP1c (Goldberg *et al.*, 1995) because of their negligible MD relaxation. Hence, our comparisons of the resulting enzyme-ligand complexes with the starting ones (see below) should actually also reflect a level of similarity/diversity with those from the former work (Gauss *et al.*, 1997; Aggen *et al.*, 1999).

Unoccupied catalytic units

The four maps for the “free” PP1c·(Zno/Mno)·PO₄³⁻ and PP2Ac·(Zno/Mno)·PO₄³⁻ catalytic units are given in Fig. 2. A summary of the enzymes’ amino-acid residues, whose C^α carbons have moved in MD by more than 5.5 Å away from their starting positions, is given in Table 2 while the sequence-averaged C^α-based root-mean-square (RMS) deviations of the final *versus* the starting snapshots in the MD simulations are given in Table 3. It is seen that the unoccupied PP1c with the Zno dication (RMS = 3.63 Å) appears to be the most flexible of all the systems under study (see below, Fig. 2 *vs.* 4–7 and Table 3) and, in particu-

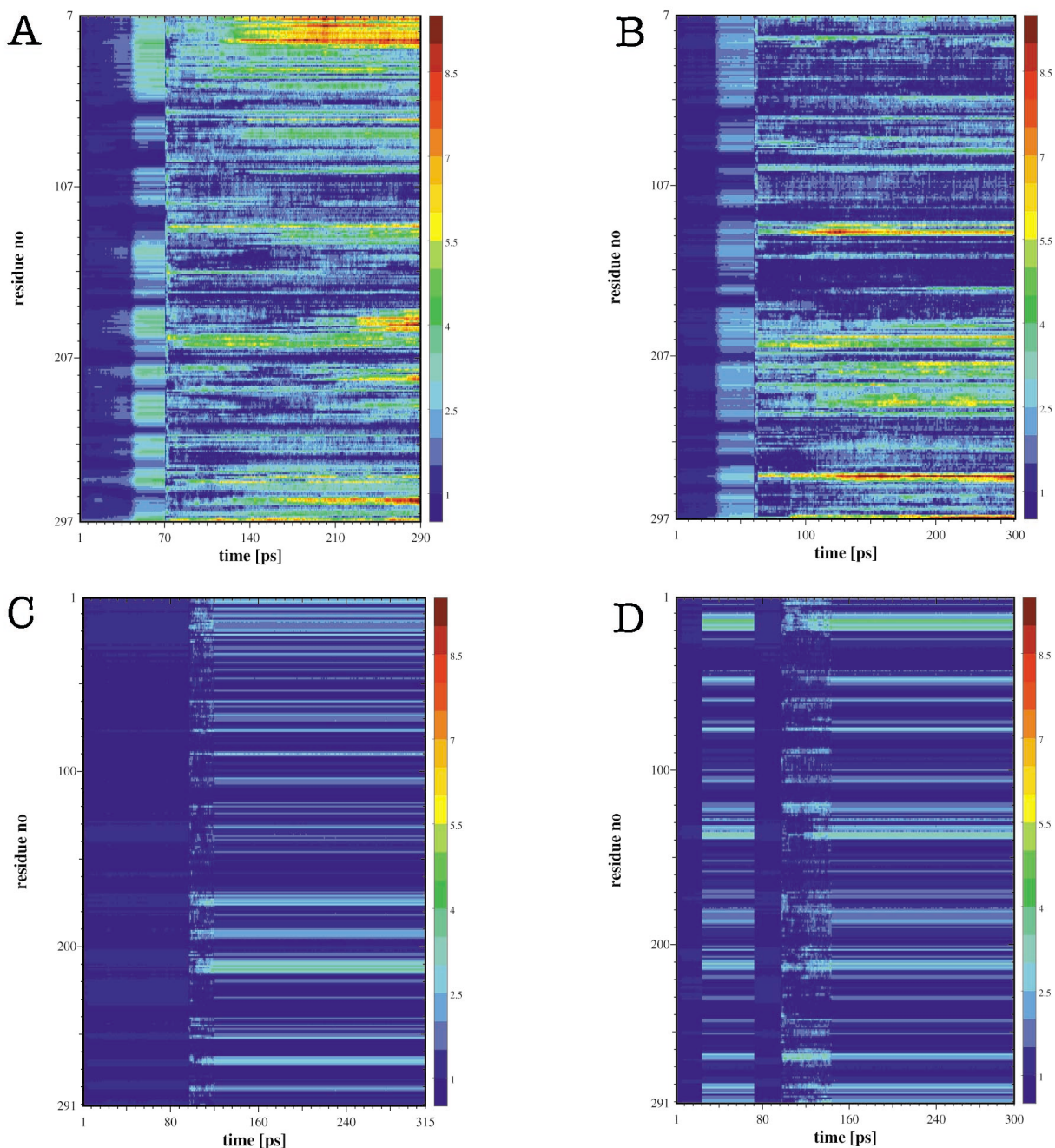


Figure 2. The contour plots typical of the collective MD trajectories in four free enzyme models:

A. PP1c·Zno·Tpo, B. PP1c·Mno·Tpo, C. PP2Ac·Zno·Tpo, D. PP2Ac·Mno·Tpo, represented by the C^α sequential positions along the vertical axes, over the time range of about 300 ps (horizontal axes). The contours are drawn every 1.5 Å, in agreement with the color scale defined on the right. They denote departure, evolving in time, of any C^α relative to its starting position. For instance, the build-up of the green-to-orange traces for A: PP1c·Zno·Tpo and B: PP1c·Mno·Tpo between residues 128–136 corresponds to a flapping-down movement of helix D due to the $D\alpha$ - $E\alpha$ hinge towards the trough of the hydrophobic groove, see text.

lar, it is more flexible than the PP1c with the Mno indication (RMS = 2.65 Å). Surprisingly, the unoccupied PP2Ac models with both the Zno and Mno

indications appear much less flexible than their PP1c counterparts (RMS = 1.43 Å and 1.51 Å, respectively). This is even more surprising if one re-

Table 2. A summary of the motional characteristics of the models under study^a

Ligand Type	Zno dication			Mno dication			Common for Zno and Mno dication		
	PP1		PP2A	PP1		PP2A	PP1	PP2A	
Unoccupied catalytic domain	7-12 13 14-15 16 17-26 34-36 37-44 45-47 55-57 62-63 68 194-200	69 72-78 86 96-98 130-141 132-142 179 180-173 184-185 186 187 300-end	212-216 217-221 222-223 226 230-237 255 274-277 276 279-287 287-292 296-298	209-215	7-9 20 23-27 55-57 68 86-89 130 132-137 168 175-176 178-180 185-202	196 210-214 222-227 229-231 233 234-237 239-242 261-262 276-280 300-end	14-20 136-138 210-211	7-9 23-26 274-276 300-end 68 86 130 132-137 179-180 185-187 196 212-214 222-223, 226 230, 233, 237	210-211
DAR inhibitor sequence	7-11 12-21 22-25 26-28 82-94 197-200 220-236	274-278 287-289 299-302 303-305	2-3 6-9 14 16-18 135-139 265 266-269 292-293	22-28 31-39 98 137-139 142-146 147-154 193-200 212-214	218-220 298-306 307 308-end 230-231 239-241 261 273-277 287-292	6-12 14 15-20 136-140 172, 174 176-177 208-219 251 263-265 282	21-28 197-200 220, 222-226 228-231 273-278 287-289 298-302 303-305	6-9 14 16-18 135-139 265	
I-1 inhibitor sequence	32-37 195 199-200 275 276-278 288 289-290 291-292 302-303 304 307-end		1-8 9-10 11-12 13-14 15-22 89-93 124-127 173-178 210-218 298-301 302-end	22 23-27 95-98 196-201 219-227 232-237 239-242 276-278 287-292 300-303 312-end	22-27 222-227	7-10 12-14 14-21 131-133 135-140 189-190 211-217 292 300-end	195-196 199-200 275-278 288-292 302-303 307-end	7-21 211-217 302-end	
7-pep PP2Ac-selective substrate	22-27 80-86 130-137 194-201 210-220 222-227	224 233-237 264-267 275-277 299-303 304-305	13-18 23-24 171-173 189-191 266 292-293	17-27 128-129 132-137 167-170 182 197-206	222-227 261 274-275 287-292 298-303	292-293	22-27 130-130 194-201 222-227 261 274-275 299-303	292-293	
I1-pep PP1c-selective substrate	25 21-27 96-98 147-149 180-196 194-195	198-205 213-214 215-217 220-227 231-237 242	253-257 259-263 260 290-291 300-302 310-end	123-126 202-204 209-211 211 213-215 265-270 289-292	14-25 168 180-185 195-196 197-200 132-133 134-135 136	222-223 228-236 252-257 259-273 211-213 278 287-289 299-302 310-312	6 59-60 89 137-138 189-192 292-294 213-217 222-223 228-236	21-25 253-257 98 180-185 195-196 198-200 213-217 222-223 228-236	292
Common for DAR and I-1	195 199-200 275-278 288-289 302-304		2-9 14-18	22-27 196-200 219-220 222-227	239-241 276-277 287-292 300-303	6-10 14-20 136-140 211-217	199-200 276-277 288 302-303	6-9 14-18	
Common for the substrate sequences	22-27 194-195 198-201 213-217	220-227 233-237 300-302	-	17-25 168 182 197-200	222-223 261 287-289 299-302	292-293	21-25 198-200 222-223 300-302	-	

^aThe summary is based on the complete set of 20 trajectory maps, subject of this work. The four maps for the “free” domains PP1c·Zno(Mno)·PO₄³⁻ and PP2Ac·Zno(Mno)·PO₄³⁻ are given in Fig. 2. Those for the four peptide ligands DAR, I-1, 7-pep and 11-pep, each in the combinations of the PP1c and PP2Ac enzyme pairs with either Zno or Mno dications, are given as the consecutive sets of four maps in Figs. 3–6, respectively. All enzymes’ residues whose C^α atoms have fluctuated in MD by more than 5.5 Å away from the starting positions are included in the Table and those whose C^α atoms have fluctuated by more than 7.5 Å are marked in bold. In addition, the last two columns indicate the motions common for the Zno and Mno-comprising PP1c and PP2Ac protein models, while the last two rows indicate the motions common for both inhibitor–enzyme and the both substrate–enzyme complexes.

Table 3. The sequence-averaged C^α -based RMS deviations between the final and the starting snapshots in the MD simulations of the systems studied^{a,b}

Ligand Type	Zno dication		Mno dication	
	PP1	PP2A	PP1	PP2A
Unoccupied enzyme	3.633	1.429	2.650	1.505
	290	315	300	300
DAR	2.517	1.676	2.709	1.786
	290	270	300	270
I-1	2.133	1.959	2.307	1.858
	260	270	330	270
7-pep	2.136	1.497	2.160	1.577
	260	270	370	270
11-pep	2.706	1.586	2.819	1.644
	280	270	320	286

^aThe upper values: RMS in Å. ^b The lower values: MD total time(s) in ps.

alizes that the PP1c model of the free enzyme is based on the experimental structure of the covalent PP1c-inhibitor complex (Goldberg *et al.*, 1995), while the PP2Ac unit is clearly homology-modeled from the PP1c template. Furthermore, while the experimental starting model of PP1c comprised six structural water molecules, the homology-modeled PP2Ac was devoid of this wa-

is, by homology, defined by their respective counterparts: D57, H59, D85, D88, R89, N115, H116, H165, D200, R212, H239 and Y263 (Goldberg *et al.*, 1995). It is seen that none of these residues are listed in Table 4 for either free PP1c or PP2Ac. This is confirmed by the low RMS values in Table 4 between the starting and the relaxed geometries of the active centers of the two enzymes.

Table 4. The matrix of the C^α -based RMS deviations among the starting and the MD-relaxed active center geometries of the four ligand-free, PO_4^{3-} -bound PP1c and PP2Ac units with either Zno or Mno dications^a

	PP1c·Zno	PP1c·Mno	PP2Ac·Zno	PP2Ac·Mno
PP1c·Zno	1.886 ^b	1.730	2.030	1.783
PP1c·Mno		1.356 ^b	1.783	1.504
PP2Ac·Zno			1.053 ^b	0.910
PP2Ac·Mno				1.178 ^b

^aRMS in Å. ^bThe values relating to the differences between the respective starting and MD-relaxed configurations are on the diagonal.

ter. However, inspection of the four fully relaxed PP2Ac variants demonstrated that they accommodated 3–4 structural water molecules in the sites analogous to those in PP1c. In these four variants of unoccupied enzyme units, the relaxed active centers are well conserved. This can be inferred from a careful inspection of the data in Table 2, keeping in mind that the PP1c active center is defined by the following 12 residues: D64, H66, D92, D95, R96, N124, H125, H173, D208, R221, H248 and Y272, and the probable PP2Ac active center

The deviations between the starting and the relaxed configurations range from 1.05 Å for PP2Ac·Zno· PO_4^{3-} to 1.89 Å for PP1c·Zno· PO_4^{3-} (see the diagonal in Table 4) and the deviations between the relaxed configurations range from 0.91 Å (for PP2Ac·Zno· PO_4^{3-} vs. PP2Ac·Mno· PO_4^{3-}) to 2.03 Å (for PP1c·Zno· PO_4^{3-} vs. PP2Ac·Zno· PO_4^{3-}), compare the upper triangle in Table 4. The most poorly and most closely overlapping free-enzyme active centers are shown in Fig. 3.

Ligand-substituted catalytic units

The MD trajectories for the enzymes docking four peptide ligands DAR, I-1, 7-pep and 11-pep, each in the combinations of the PP1c and PP2Ac enzyme pairs with either Zn or Mn dications, are given as the consecutive sets of four maps in Figs. 4–7, respectively. A summary of the enzymes amino-acid residues, whose C $^{\alpha}$ carbons have moved in MD by more than 5.5 Å away from their starting positions, is continued in Table 2. The sequence-averaged C $^{\alpha}$ -based RMS deviations of the final snapshots from the starting ones in the MD simulations are given in Table 3. The last two columns in Table 2 indicate the motions common for the Zn and Mn-comprising PP1c and PP2Ac, while the last two rows indicate the motions common for the two inhibitor–enzyme and the two substrate–enzyme complexes. As can be seen from Table 3, greater flexibility in the PP1c than in the PP2Ac complexes is regularly observed, which is easy to infer from the comparison(s) among the relevant RMS values in Table 3 and among the relative numbers of amino-acid residues experiencing excessive motions in specific PP1c–ligand complexes *versus* PP2Ac–ligand complexes, as demonstrated in Table 2 and Figs. 4–7. No significant differences in the motional characteristics between the Zn- and Mn-comprising catalytic units were observed, irrespective whether it was the PP1c or PP2Ac catalytic unit. Contrary to the overall flexibilities, the relaxed active centers are usually well conserved, which is confirmed by the relatively low RMS values (Table 5), being a measure of similarities among the 16 relaxed and starting active center configurations simultaneously for both PP1c and PP2Ac complexes. The deviations between the starting and the relaxed configurations range from 0.84 Å for the PP1c·Mn·DAR complex to 2.62 Å for the PP1c·Mn·I-1 complex (see the diagonal in Table 5) and those among the relaxed configurations range from 0.66 Å between the PP2Ac·Zn·7-pep and PP2Ac·Mn·I-1 complex to 2.06 Å between the PP1c·Zn·7-pep and PP2Ac·Mn·11-pep complex (see the upper triangle in Table 5). The differences between the free and the ligand-occu-

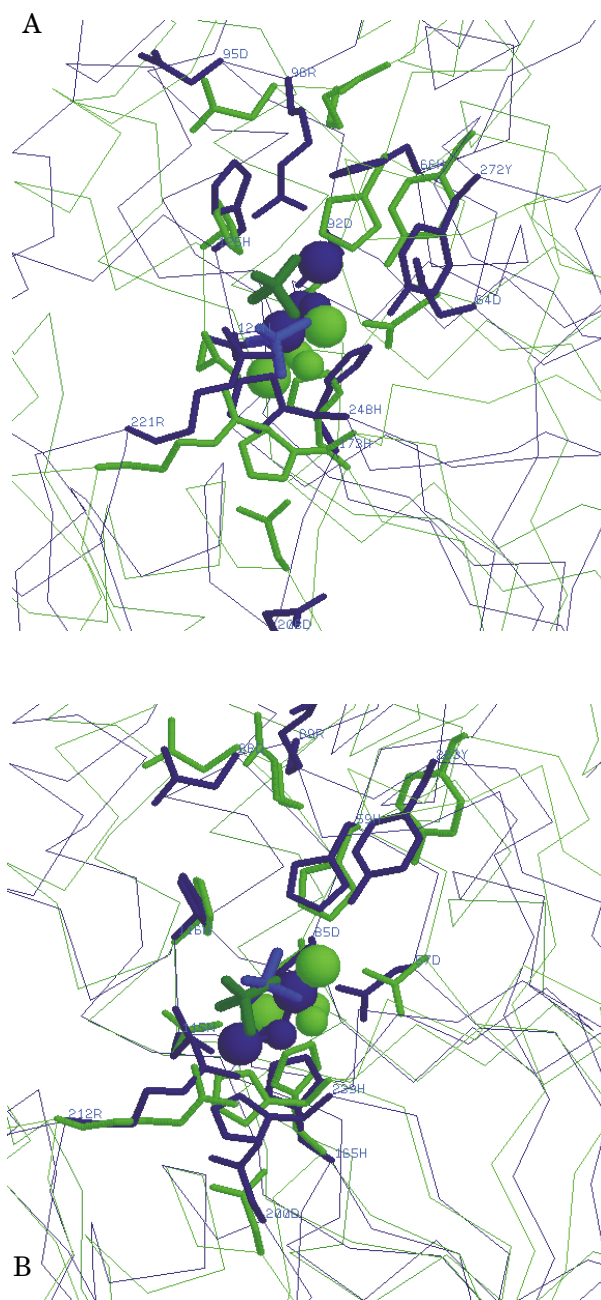


Figure 3. The overlapping active centers with key residues labeled and shown as sticks and the protein chains shown as thin backbones.

A: The worst fit corresponding to RMS = 2.03 Å for PP1c·Zn·Tpo (blue) *vs.* PP2Ac·Zn·Tpo (green) and labeled in accordance with the PP1c sequence. B: The best fit corresponding to RMS = 0.91 Å for PP2Ac·Zn·Tpo (blue) *vs.* PP2Ac·Mn·Tpo (green) and labeled in accordance with the PP2Ac sequence.

piated active centers, although not shown, are of a comparable order.

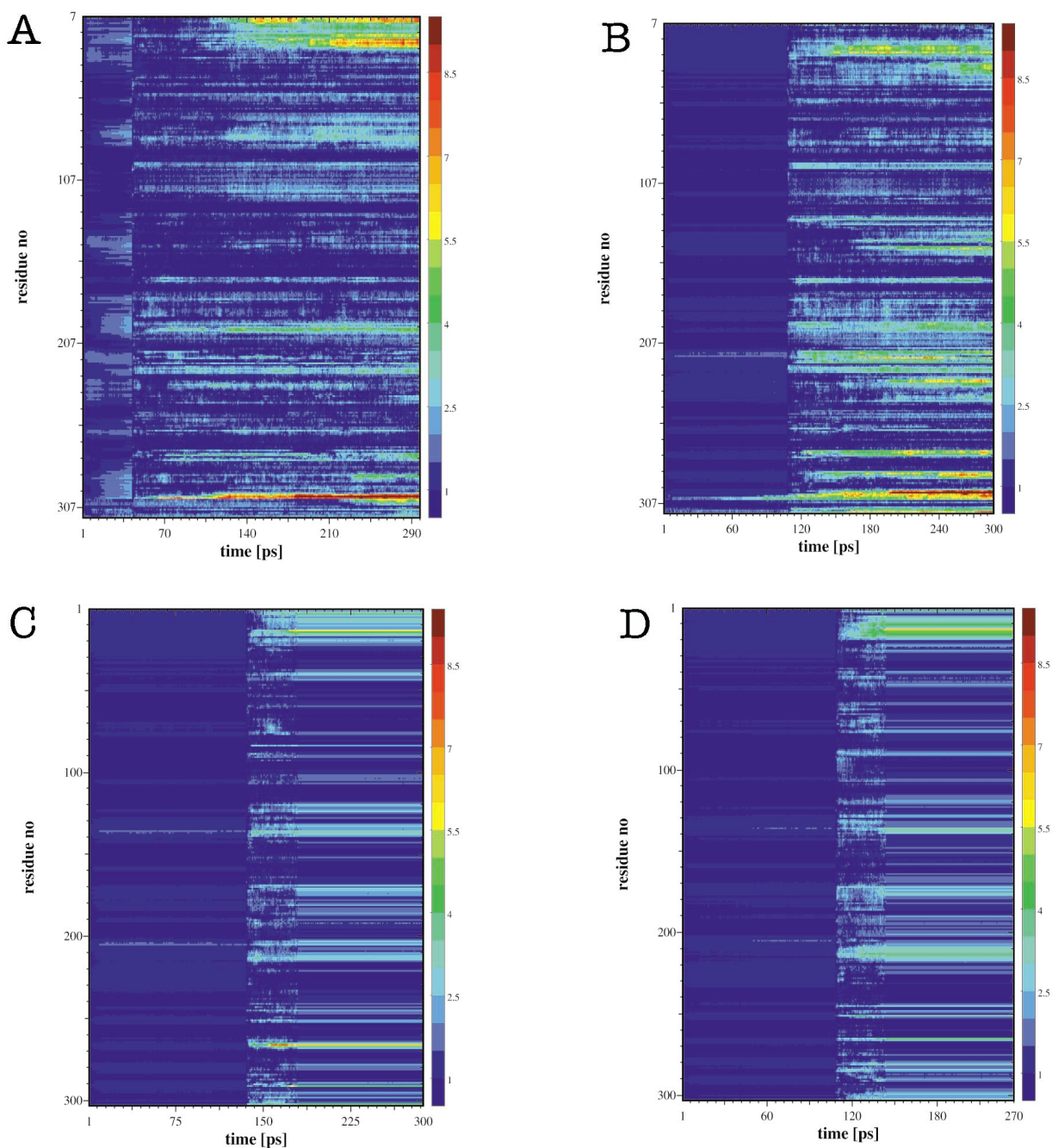


Figure 4. The contour plots typical of the collective MD trajectories in four enzyme models with the DARPP-32 dodecapeptide sequence docked.

A. PP1c·Zno·DAR, B. PP1c·Mno·DAR, C. PP2Ac·Zno·DAR, D. PP2Ac·Mno·DAR. For details, see legend to Fig. 2.

DISCUSSION

From the inspection of Figs. 2 and 4–7 one can easily see the time points at which the (Zn/Mno)·(phosphate/ligand) constraints (at 60–90 ps) were released (see Methods). The re-

laxed structures of the free PP1c units, either with Zn²⁺ or Mn²⁺ dication center in the active sites differ to a considerable extent from the starting (x-ray) structure of PP1c (see Tables 2, 3 and Figs. 2A and 2B). Apart from the PP1c N- and C-termini, the most significant differences and ac-

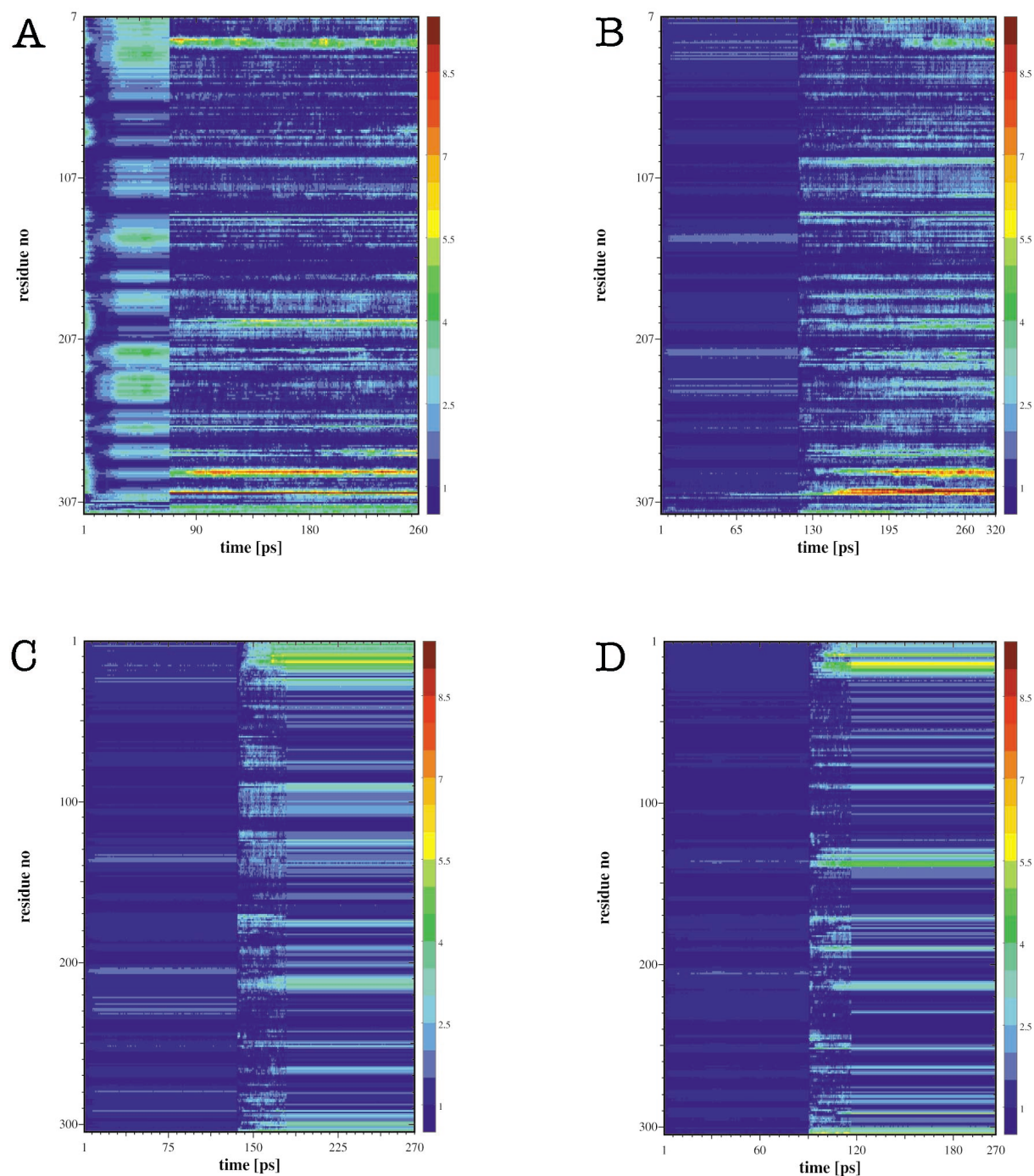


Figure 5. The contour plots typical of the collective MD trajectories in four enzyme models with the Inh-1 tridecapeptide sequence docked.

A. PP1c·Zno·I-1, B. PP1c·Mno·I-1, C. PP2Ac·Zno·I-1, D. PP2Ac·Mno·I-1. For details, see legend to Fig. 2.

companying changes have affected the three external and mutually proximal PP1c sections surrounding the active center and including the neighboring parts of the substrate cleft. Using the notation introduced in Goldberg *et al.* (1995), the changes for the PP1c·Zno·PO₄³⁻ consist: (i) he-

lix D and the associated α D- α E loop (residues 128–136); (ii) helix G and the N-terminal part of the α G- α H loop, flanking the lower edge of the C-terminal end of the hydrophobic groove (residues 180–192); and (iii) the N-terminal half of the loop between β 8- β 9 strands (residues 217–220),

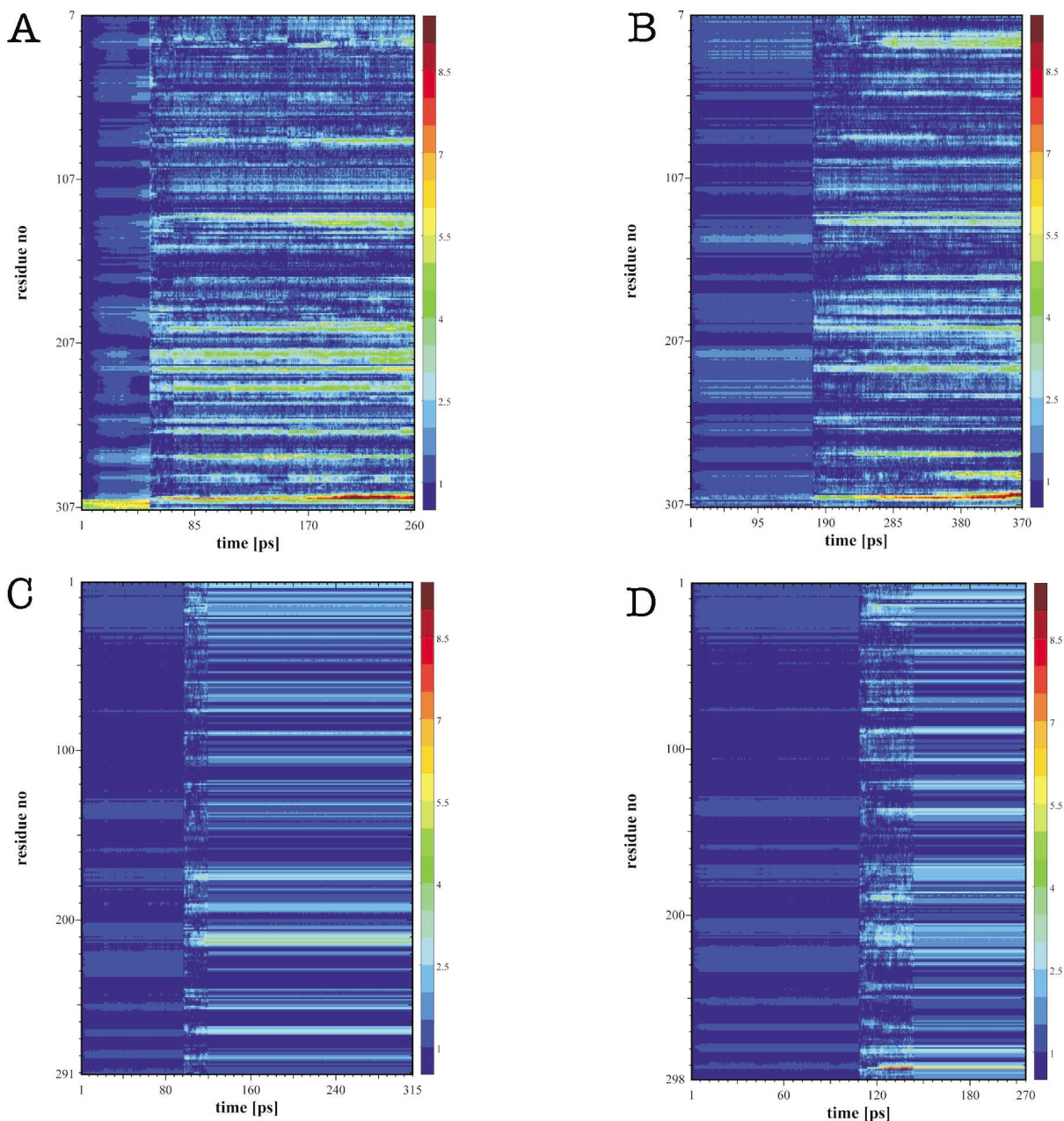


Figure 6. The contour plots illustrating the evolution of the geometry in four enzyme models with the heptapeptide PP2Ac-selective substrate docked.

A. PP1c·Zno·7-pep, B. PP1c·Mno·7-pep, C. PP2Ac·Zno·7-pep, D. PP2Ac·Mno·7-pep. For details, see legend to Fig. 2.

flanking the lower edge of the acidic groove (compare Fig. 2A against Fig. 1; see also Table 2 and Woźniak *et al.*, 2000). The most variable residue ranges in PP1c·Mno·PO₄³⁻ (compare Fig. 2B against Fig. 1; see also Table 2 and Woźniak *et al.*,

2000) were similar to those in PP1c·Zno·PO₄³⁻ although the changes were less spectacular. While in the microcystin-bound PP1c the hydrophobic trench is filled with the long side-chain of the Adda (Goldberg *et al.*, 1995) residue from the

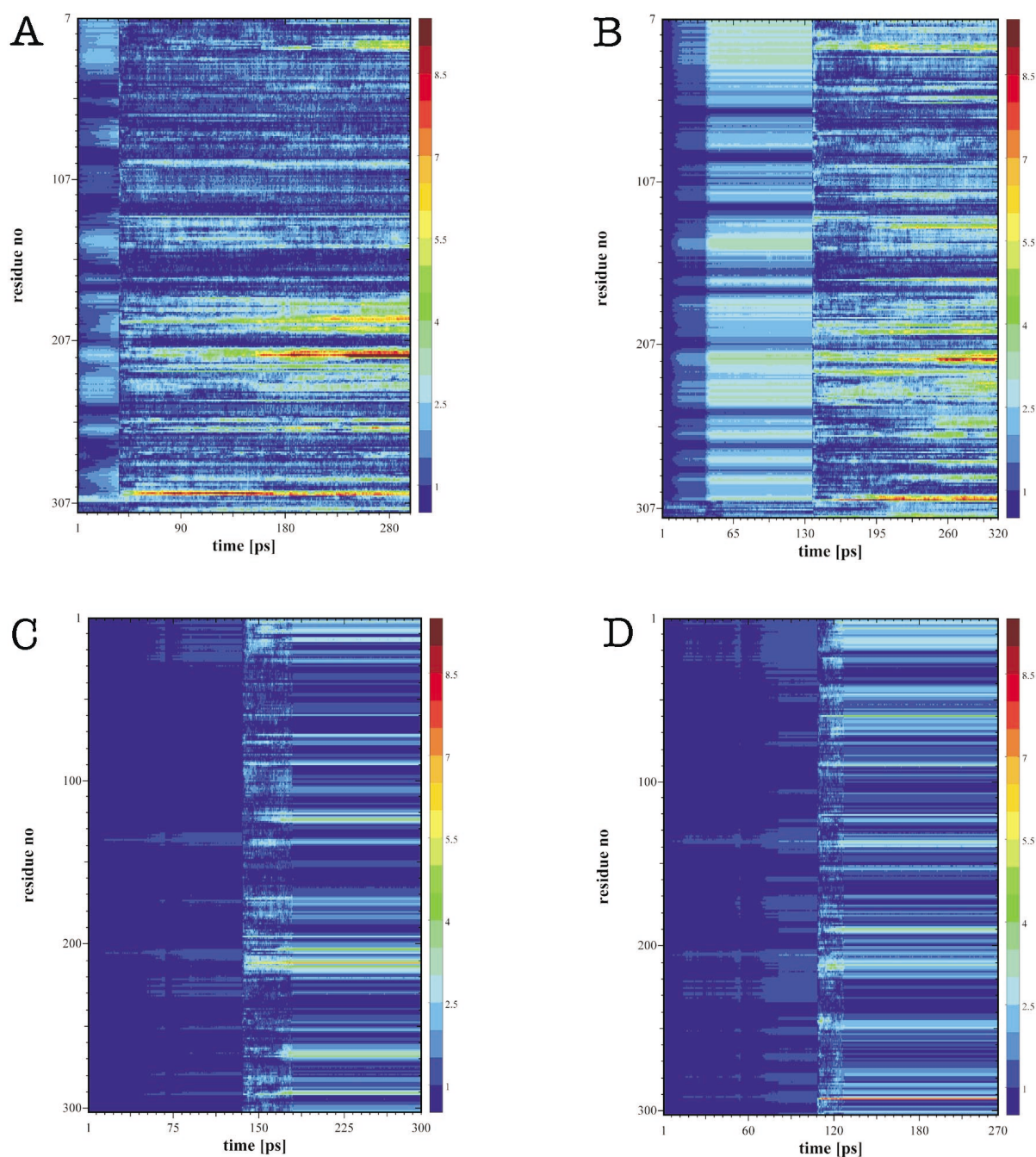


Figure 7. The contour plots illustrating the evolution of the geometry in four enzyme models with the undecapeptide PP1c-selective substrate docked.

A. PP1c·Zno·11-pep, B. PP1c·Mno·11-pep, C. PP2Ac·Zno·11-pep, D. PP2Ac·Mno·11-pep. For details, see legend to Fig. 2.

toxin, here the empty hydrophobic groove gets partly filled with the dropping helix D due to a hinge-like feature of the α D- α E loop. Helix D, while lowered towards the hydrophobic trough, may cause helix G with the α G- α H loop, and the

β 8- β 9 loop on the opposite sides of itself to move and deform most extensively (cf. Fig. 1). Interestingly, the pattern of interactions between Zno/Mno and the conserved residues pointed out above is essentially unperturbed (not shown).

Table 5. The matrix of the C^α-based RMS deviations among the starting and the MD-relaxed active center geometries of the four ligand-bound PP1c and PP2Ac units with either Zn or Mn dications^a.

		PP1c·Zno				PP2Ac·Zno				PP1c·Mno				PP2Ac·Mno			
		DAR	11-pep	7-pep	I-1	DAR	11-pep	7-pep	I-1	DAR	11-pep	7-pep	I-1	DAR	11-pep	7-pep	I-1
PP1c ·Zno	DAR	1.071 ^b	1.166	1.587	1.284	0.996	1.522	1.068	<i>0.986</i>	0.885	1.503	1.118	1.105	0.920	1.235	0.858	1.379
	11-pep		1.299 ^b	1.122	0.989	1.043	1.568	0.985	1.305	1.056	1.042	1.440	0.911	1.198	1.606	0.988	1.272
	7-pep			1.574 ^b	1.544	1.407	2.038	1.396	1.777	1.259	0.999	1.775	1.589	1.581	2.056	1.456	1.615
	I-1				1.409 ^b	1.420	1.479	1.250	1.263	1.236	1.404	1.476	1.095	1.384	1.335	1.097	1.550
PP2Ac ·Zno	DAR					<i>0.941^b</i>	1.346	1.027	1.185	0.915	1.386	1.153	0.922	0.838	1.490	0.911	1.200
	11-pep						1.603^b	1.790	1.364	1.384	1.734	1.305	1.007	1.300	1.243	1.211	1.890
	7-pep							1.032 ^b	1.201	1.030	1.518	1.392	1.317	1.011	1.504	1.064	<i>0.658</i>
	I-1								1.454 ^b	1.219	1.657	1.010	1.111	0.899	1.485	0.944	1.447
PP1c ·Mno	DAR								<i>0.843^b</i>	1.159	1.199	1.077	0.956	1.246	<i>0.673</i>	1.169	
	11-pep									1.483 ^b	1.699	1.521	1.518	1.884	1.362	1.676	
	7-pep											1.650 ^b	1.122	1.014	1.365	0.917	1.527
	I-1												2.622^b	1.089	1.275	0.835	1.616
PP2Ac ·Mno	DAR													1.205 ^b	1.288	0.810	1.093
	11-pep														1.410 ^b	1.186	1.662
	7-pep															1.119 ^b	1.290
	I-1																1.261 ^b

^aRMS in Å. The maximum and the minimum values typical of each of three sub-blocks (framed): (PP1 or PP2A)·Zno, (PP1 or PP2A)·Mno and (PP1 or PP2A)·(Zno or Mno) are given in bold and italics, respectively. This also applies to the diagonal, subdivided into two sets depending on which dication (Zno or Mno) is incorporated in the enzyme. ^bThe values relating to the differences between the respective starting and MD-relaxed configurations are on the diagonal.

Contrary to the free PP1c subunits, the complexed PP1c structures, both with the Zn or Mn dication center in the active sites, very little differ from the starting (x-ray) structure of PP1c (see Figs. 4AB–7AB). For instance, in the PP1c·Zno·DAR complex, apart from the N-terminal prosegment and the C-terminus, the only noticeable motion (up to 3.5 Å) is experienced by Asp197-Glu198 in the C-terminal section of the α G- α H loop (see Fig. 4A vs. Fig. 1 and Table 2). Similarly, the pattern of interactions between Zn/Mno and the conserved residues, and the orientation of the di-nuclear ion center relative to “canonical” orientation observed in the crystal structures (Egloff *et al.*, 1995; Griffith *et al.*, 1995; Kissinger *et al.*, 1995) remain essentially unperturbed (not shown). The relaxed DAR and I-1 inhibitor ligands comply with the demand for, on the one hand, good interactions between their four Arg residues and the acidic groove and, on the other, for packing their mainly non-polar C-termini in the hydrophobic groove (Goldberg *et al.*, 1995). However, the detailed interactions between any specific peptide ligand and the PP1c·Zno vs. the same ligand and PP1c·Mno model differ considerably (not shown).

As concern the PP2Ac·(Zno/Mno) models of unknown experimental structure, they were modeled *via* homology on the framework of PP1c,

given the 49% sequence identity shared between the two catalytic units (Dawson & Holmes, 1999). Despite this high homology, PP2Ac essentially loses most of the acidic character in the groove termed “acidic” in PP1c (Goldberg *et al.*, 1995), as a result of the following four amino acid replacements lining the floor of this groove: D220P in PP1c numbering (or D211P in the PP2Ac numbering) in the β 8- β 9 loop, E252M (E243M) in the β 10- β 11 loop, E256N (E247N) in the β 11 sheet and A259H (A250H) in the β 11- β 12 loop (cf. Fig. 1). One should expect this dramatic change of properties to significantly affect the binding of the four ligands, comprising 2 (7-pep) to 4 (11-pep, I-1 and DAR) basic Arg and/or Lys residues at their N-termini. In particular, they should appear to bind more loosely the enzyme with these termini. In this respect, it is surprising that both the free PP2Ac·(Zno/Mno)·PO₄³⁻ catalytic units and those associated with the peptide ligands, exhibit much less flexibility, including the motion of the ligands, in comparative MD simulations than their PP1c counterparts (cf. Figs. 2CD, 4CD–7CD with Figs. 2AB, 4AB–7AB, respectively). Judging upon the total structure alterations as measured by the RMS values listed in Table 3 and 4, and on the active-center deformations as measured by selected sets of the RMS values in Tables 4, one can see, with reference to the D and C sets of trajec-

tory maps in Figs. 2, 4–7, that the PP2Ac structures, irrespective of the metal dication and ligand, undergo but small changes in the simulations. This is also clearly seen in Table 2 in the scarce occurrence of PP2Ac residues experiencing deviations from the starting structures larger than 5.5 Å, limited only to some residues from extra-globular loops. This feature can hardly be reconciled with any differences in biological selectivity of the ligands towards PP1c *vs.* PP2Ac catalytic units.

Currently, it is believed that a combination of Zn²⁺ and Fe²⁺ (Cohen, 1997; Chu *et al.*, 1996) is a probable candidate for the PP1c di-cation center *in vivo*. While we have currently been working on such a dication·OH⁻ complex, in view of this work one can doubt that even a properly parameterized pseudomolecule “ZnFeO” could account for subtleties pertinent to the proper choice of the cation(s) and its detailed role in the PP1c mechanism, let alone PP2Ac whose structure is only a “qualified guess” in this work. In view of the rapidly growing evidence (over 600 hundred papers per year) on the regulatory mechanisms of the protein phosphatases it becomes clear that, apart of the metal di-cation type, an essential role is attributed to the abundance of variable regulatory protein units, depending on specific tissues and targeting the catalytic units to specific tasks. For instance, a complex mode of binding of the DARPP-32 and Inh-1 inhibitors to PP1c has been proven recently. Both DARPP-32 and Inh-1 involve multiple sequence fragments for high affinity and selectivity (Endo *et al.*, 1996; Kwon *et al.*, 1997; see also introduction) binding to different sites on PP1c (Huang *et al.*, 1999). Apart from the sequence involving pThr and its surroundings, there is still a short KIQF sequence close to the N-terminus (8–12 in Inh-1 and 7–11 in DARPP-32) which is a requisite for their binding and selectivity. Furthermore, this motif is more or less conserved in a quite wide spectrum of diverse PP1c regulatory units (Aggen *et al.*, 2000). A volatile binding of the phosphorylated dodecapeptide in the catalytic groove may thus argue for a complex mechanism for binding Inh-1 and DARPP-32 to PP1c, involving in a cooperative way at least two distal sequence fragments.

In this work we introduced the test case Zno and Mno pseudo-molecules (-residues), composed of an either Zn²⁺ or Mn²⁺ dication center, respectively, nesting a structural OH⁻ nucleophile between the metal nuclei, so that the total charge of either Zno or Mno was +3. For their incorporation into the AMBER force field, Zno and Mno were structurally optimized and parameterized using advanced *ab initio* methodology so as to meet geometrical, mechanical and electrostatic requirements (see Fig. 2 in Methods), typical of the crystal structures of PP1c. Our results demonstrate that both Zno and Mno behave well in typical MD simulations and thus prove the concept of pseudomolecules to be useful. Simultaneously, the differences between Zno and Mno, as reflected in the parameterization, seem to be not precise enough for being specifically accented in the respective simulations.

REFERENCES

- Aggen, J.B., Humphrey, J.M., Gauss, C.-M., Huang, H.-B., Nairn, A.C. & Chamberlin, A.R. (1999) The design, synthesis and biological evaluation of analogues of the serine-threonine protein phosphatase 1 and 2A selective inhibitor microcystin LA: rational modifications imparting PP1 selectivity. *Bioorg. Med. Chem.* **7**, 543–564.
- Aggen, J.B., Nairn, A.C. & Chamberlin, R. (2000) Regulation of protein phosphatase 1. *Chem. & Biol.* **7**, R13–R23.
- Barford, D. (1996) Molecular mechanisms of the protein serine/threonine phosphatases. *Trends Biochem. Sci.* **21**, 407–412.
- Bayly, C.I., Cieplak, P., Cornell, W.D. & Kollman, P. (1993) A well-behaved electrostatic potential based method using charge restraints for deriving atomic charges: The RESP model. *J. Phys. Chem.* **97**, 10269–10280.
- Berndt, N. (1999) Protein dephosphorylation and the intracellular control of the cell number. *Front. Biosci.* **4**, 22–42.
- Bernstein, F.C., Koetzle, T.F., Williams, G.J., Meyer, E.E.J., Brice, M.D., Rodgers, J.R., Kennard, O., Shimanouchi, T. & Tsanumi, M. (1977) The protein data bank: A computer-based archive file for macromolecular structures. *J. Mol. Biol.* **112**, 535–542.

- Brooks, III, C.L., Karplus, M., & Pettitt, B.M. (1988) Proteins: A theoretical perspective of dynamics, structure, and thermodynamics, *Adv. Chem. Phys.* **71**, 1-259.
- Case, D.A., Pearlman, D.A., Caldwell, J.W., Cheatham III, T.E., Ross, W.S., Simmerling, C., Darden, T., Merz, K.M., Stanton, R.V., Cheng, A., Vincent, J.J., Crowley, M., Ferguson, D.M., Radmer, R., Seibel, G.L., Singh, U.C., Weiner, P.K. & Kollman, P.A. (1997) *AMBER, v.5.0*, University of California, San Francisco, CA, U.S.A.
- Chu, Y., Lee, E.Y.C. & Schlender, K.K. (1996) Activation of protein phosphatase 1. Formation of a metalloenzyme. *J. Biol. Chem.* **271**, 2574-2577.
- Cohen, P.T.W. (1997) Novel protein serine/threonine phosphatases: Variety is the spice of life. *Trends Biochem. Sci.* **22**, 245-251.
- Das, A.K., Helps, N.R., Cohen, P.T.W. & Barford, D. (1996) Crystal structure of the protein serine/threonine phosphatase 2C at 2.0 Å resolution. *EMBO J.* **15**, 6798-6809.
- Dawson, J.F. & Holmes, C.F.B. (1999) Molecular mechanisms underlying inhibition of protein phosphatases by marine toxins. *Front. Biosci.* **4**, D646-658.
- Egloff, M.P., Johnson, D.F., Moorhead, G., Cohen, P.T.W., Cohen, P. & Barford, D. (1997) Structural basis for the recognition of regulatory subunit by the catalytic subunit of protein phosphatase 1. *EMBO J.* **16**, 1876-1887.
- Egloff, M.P., Cohen, P.T., Reinemer, P. & Barford, D. (1995) Crystal structure of the catalytic subunit of human protein phosphatase 1 and its complex with tungstate. *J. Mol. Biol.* **254**, 942-959.
- Endo, S., Zhou, X., Connor, J., Wang, B. & Shenolikar, S. (1996) Multiple structural elements define the specificity of recombinant human inhibitor-1 as a protein phosphatase-1 inhibitor. *Biochemistry* **35**, 5220-5228.
- Gauss, C.-M., Sheppeck, J.E., Nairn, A.C. & Chamberlin, R. (1997) A molecular modeling analysis of the binding interactions between the okadaic acid class of natural product inhibitors and the Ser-Thr phosphatases, PP1 and PP2. *Bioorg. Med. Chem.* **5**, 1751-1773.
- Goldberg, J., Huang, H., Kwon, Y., Greengard, P., Nairn, A.C. & Kuriyan, J. (1995) Three-dimensional structure of the catalytic subunit of protein serine/threonine phosphatase-1. *Nature* **376**, 745-753.
- Griffith, J.P., Kim, J.L., Kim, E.E., Sintchak, M.D., Thomson, J.A., Fitzgibbon, M.J., Fleming, M.A., Caron, P.R., Hsiao, K. & Navia, M.A. (1995) X-ray structure of calcineurin inhibited by the immunophilin-immunosuppressant FKBP12-FK506 complex. *Cell* **82**, 507-522.
- Herzig, S. & Neuman, J. (2000) Effects of serine/threonine protein phosphatases on ion channels in excitable membranes. *Physiol. Rev.* **80**, 173-210.
- Hoops, S.C., Anderson, K.W. & Merz, K.M., Jr. (1991) Force-field design for metalloprotein. *J. Am. Chem. Soc.* **113**, 8262-8270.
- Huang, F.L. & Glinsmann, W.H. (1976) Separation and characterization of two phosphorylase phosphatase inhibitors from rabbit skeletal muscle. *Eur. J. Biochem.* **70**, 419-426.
- Huang, H.-B., Horiuchi, A., Watanabe, T., Shih, S.-R., Tsay, H.-J., Li, H.-C., Greengard, P. & Nairn, A.C. (1999) Characterization of the inhibition of protein phosphatase-1 by DARPP-32 and inhibitor-2. *J. Biol. Chem.* **274**, 7870-7878.
- Ingebritsen, T.S. & Cohen, P. (1983) Protein phosphatases: Properties and role in cellular regulation. *Eur. J. Biochem.* **132**, 255-261.
- Jia, Z. (1997) Protein phosphatases: Structures and implications. *Biochem. Cell Biol.* **75**, 17-26.
- Jorgensen, W.L., Chandrasekhar, J., Madura, J.D., Impey, R. & Klein, M.L. (1983) Comparison of simple potential functions for simulating liquid water. *J. Phys. Chem.* **79**, 926-935.
- Kissinger, C.R., Parge, H.E., Knighton, D.R., Lewis, C.T., Pelletier, L.A., Tempczyk, A., Kalish, V.J., Tucker, K.D., Showalter, R.E., Moomaw, E.W., Gastinel, L.N., Habuka, N., Chen, X., Maldonado, F., Baker, J.E., Bacquet, R. & Villafranca, J.E. (1995) Crystal structure of human calcineurin and the human FKBP12-FK506- calcineurin complex. *Nature* **378**, 641-644.
- Klee, B.C., Ren, H. & Wang, X. (1998) Regulation of the calmodulin-stimulated protein phosphatase, calcineurin. *J. Biol. Chem.* **273**, 13367-13370.
- Koradi, R., Billeter, M. & Wüthrich, K. (1996) MOLMOL: A program for display and analysis of macromolecular structures. *J. Mol. Graphics* **14**, 51-55.
- Kwon, Y.G., Huang, H.-b., Desdouits, F., Girault, J.A., Greengard, P. & Nairn, A.C. (1997) Characterization of the interaction between DARPP-32 and protein phosphatase 1 (PP-1): DARPP-32 peptides antagonize the interaction of PP-1 with binding proteins. *Proc. Natl. Acad. Sci. U.S.A.* **94**, 3536-3541.
- Lee, S., Kim, J., Park, J.K. & Kim, K.S. (1996) Ab initio study of the structures, energetics, and spectra of Aquazinc(II). *J. Phys. Chem.* **100**, 14329-14338.

- Lindvall, M.K., Pihko, M. & Koskinen, A.M.P. (1997) The binding mode of calyculin A to protein phosphatase-1. A novel spiroketal vector model. *J. Biol. Chem.* **272**, 23312–23316.
- Merz, K.M. (1991) CO₂ binding to human carbonic anhydrase-II. *J. Am. Chem. Soc.* **113**, 406–411.
- Millward, T.A., Żoźnierowicz, S. & Hemmings, B.A. (1999) Regulation of protein kinase cascades by protein phosphatase 2A. *Trends Biochem. Sci.* **24**, 186–191.
- Sayle, R. (1996) Rasmol Molecular Graphics, version 2.6, Glaxo Wellcome Research and Development, Stevenage, Hertfordshire, U.K.
- Schmidt, M.W., Baldrige, K.K., Boatz, J.A., Elbert, S.T., Gordon, M.S., Jensen, J.H., Koseki, S., Matsunaga, N., Nguyen, K.A., Su, J.S., Windus, T.L., Dupuis, M. & Montgomery, J.A. (1993) General atomic and molecular electronic structure system *J. Comput. Chem.* **14**, 1347–1363.
- SYBYL 6.2 (1996) Tripos Inc., 1699 South Hanley Rd., St. Lois, Mo. 63144, U.S.A.
- Toh, K.K.H. (1995) PlotMTV Program, Ver. 1.4.1–16 Copyright: (C); e-mail: ktoh@td2cad.intel.com.
- Williams, K.R., Hemmings, H.C. Jr., Lopresti, M.B., Konigsberg, W.H. & Greengard, P. (1986) DARPP-32: Primary structure and homology with protein phosphatase inhibitor-1, *J. Biol. Chem.* **261**, 1890–1903.
- Woźniak, E., Ołdziej, S. & Ciarkowski, J. (2000) Molecular modeling of the catalytic domain of serine/threonine phosphatase with the Zn⁺² and Mn⁺² di-nuclear ion centers in the active site. *Comp. & Chem.* **24**, 381–390.
- Żoźnierowicz, S. & Hemmings, B.A. (1996) Protein phosphatases on the piste. *Trends Cell Biol.* **6**, 359–362.